

Manuscript version: Author's Accepted Manuscript

The version presented in WRAP is the author's accepted manuscript and may differ from the published version or Version of Record.

Persistent WRAP URL:

<http://wrap.warwick.ac.uk/136422>

How to cite:

Please refer to published version for the most recent bibliographic citation information. If a published version is known of, the repository item page linked to above, will contain details on accessing it.

Copyright and reuse:

The Warwick Research Archive Portal (WRAP) makes this work by researchers of the University of Warwick available open access under the following conditions.

Copyright © and all moral rights to the version of the paper presented here belong to the individual author(s) and/or other copyright owners. To the extent reasonable and practicable the material made available in WRAP has been checked for eligibility before being made available.

Copies of full items can be used for personal research or study, educational, or not-for-profit purposes without prior permission or charge. Provided that the authors, title and full bibliographic details are credited, a hyperlink and/or URL is given for the original metadata page and the content is not changed in any way.

Publisher's statement:

Please refer to the repository item page, publisher's statement section, for further information.

For more information, please contact the WRAP Team at: wrap@warwick.ac.uk.

Mannosylated poly(ethylene imine) copolymers enhance saRNA uptake and expression in human skin explants

*Anna K. Blakney^{1,§}, Yamin Abdouni^{2,§}, Gokhan Yilmaz³, Renjie Liu², Paul F. McKay¹, Clément
R. Bouton¹, Robin J. Shattock^{1*}, C. Remzi Becer^{2,4*}*

1 Division of Infectious Diseases, Imperial College London, Norfolk Place, London W21PG, United Kingdom

2 School of Engineering and Materials Science, Queen Mary University of London, London, E1 4NS, United Kingdom

3 School of Pharmacy, University of Nottingham, Nottingham, NG7 2RD, UK

4 Department of Chemistry, University of Warwick, Coventry, CV4 7AL, United Kingdom

§ These authors contributed equally to this work

* Correspondence: remzi.becer@warwick.ac.uk and r.shattock@imperial.ac.uk

KEYWORDS

Polyethylene imine, mannose, self-amplifying RNA, gene delivery, skin explants

ABSTRACT

Messenger RNA (mRNA) is a promising platform for both vaccines and therapeutics, and self-amplifying RNA (saRNA) is particularly advantageous as it enables higher protein expression and dose minimization. Here, we present a delivery platform for targeted delivery of saRNA using mannosylated poly(ethylene imine) (PEI) enabled by the host-guest interaction between cyclodextrin and adamantane. We show that the host-guest complexation does not interfere with the electrostatic interaction with saRNA, and observed that increasing the degree of mannosylation inhibited transfection efficiency *in vitro* but enhanced the number of cells expressing GFP by 8-fold in human skin explants. Besides, increasing the ratio of glycopolymer to saRNA also enhanced the percentage of transfected cells *ex vivo*. We identified that these mannosylated PEIs specifically increased protein expression in the epithelial cells resident in human skin in a mannose-dependent manner. This platform is promising for further study of glycosylation of PEI and targeted saRNA delivery.

1. INTRODUCTION

Recent advances and investment in RNA technology has enabled messenger RNA (mRNA) to become a clinically viable platform for both vaccines and protein replacement therapeutics. Self-amplifying mRNA (saRNA) has emerged as a next-generation approach, and has several advantages compared to both mRNA and plasmid DNA (pDNA). Because saRNA vectors are derived from the alphavirus genome,¹ they are able to self-replicate in the cytoplasm, resulting in amplification of the delivered dose of RNA and a higher magnitude and duration of protein expression than mRNA.²⁻⁴ Compared to pDNA, saRNA is a minimal genetic vector and does not pose the risk of integration or insertional mutagenesis.⁵ While a number of mRNA vaccines and therapeutics are currently being tested in the clinic,⁶ there have not yet been any non-viral RNA replicons tested in human clinical trials.⁷

saRNA has previously been formulated with a variety of delivery platforms, including lipid nanoparticles (LNPs),^{8, 9} a cationic nanoemulsion,³ cationic polymers^{10, 11} and ionizable dendrimers.¹² These formulations are not tailored for targeting of certain cell populations, but rather increased overall cellular uptake and expression of the saRNA. Liang *et al.* previously observed that while neutrophils, monocytes and dendritic cells infiltrate the injection site and take up the RNA, it was mainly monocytes and dendritic cells that translated mRNA formulated in LNPs.¹³ Both siRNA and mRNA has previously been targeted to leukocytes using the Anchored Secondary scFv Enabling Targeting (ASSET) platform, in which LNPs are coated in monoclonal antibodies to target specific leukocyte subsets.¹⁴ Furthermore, siRNA has been directly conjugated to a synthetic triantennary N-acetylgalactosamine (GalNAc)-based ligand that directly targets hepatocytes *in vivo*.¹⁵ In this study, we sought a delivery platform that enabled tailoring of glycosylation without the use of expensive monoclonal antibodies or direct

conjugation to saRNA, which is much larger in size than siRNA and unlikely to be taken up by cells without complexation.

Host-guest interactions between cyclodextrin (CD) and adamantane (Ad) have been previously used as a gene delivery platform for intravenous delivery of pDNA, wherein polyethylene glycol (PEG) was conjugated to adamantane in order to reduce toxicity of a poly(ethylene imine) (PEI) formulation.¹⁶ CD and Ad are known to form a specific and stable complex in aqueous environments through the interaction between adamantane and the hydrophobic cavity of CD.¹⁷⁻¹⁹ Glycosylation of cyclodextrins has been performed previously, and allows for a facile approach for attaching a variety of glycan groups.^{19, 20} Given the ease of chemistry and biocompatibility of CD-Ad complexes, we chose this host-guest pair as a platform for glycosylation of PEI as a targeted delivery vehicle for saRNA.

Herein, we have developed a mannosylated PEI complex enabled by the host-guest interaction between CD and Ad. We designed and synthesized a library of PEI polymers with varying degrees of mannosylation. We then characterized the polymers and the polyplexes formed when complexed with saRNA for size, charge and transfection efficiency *in vitro*. After identifying the optimal ratio of PEI to saRNA, we then tested these formulations *ex vivo* in a clinically relevant human skin explant model to characterize the transfection efficiency. Finally, we observed how the degree of mannosylation and ratio of polymer to saRNA affected cellular expression and identify of which cellular subsets are targeted.

2. MATERIALS AND METHODS

2.1. Materials

PEI MAX (Transfection grade linear polyethylenimine hydrochloride, MW 40,000) was purchased from Polysciences, Inc. Dry triethylamine (TEA) ($\geq 99.5\%$) equipped with septum,

1-adamantane carbonyl chloride and CuBr_2 were purchased from Sigma Aldrich and used as received. Tris(2-(dimethylamino)ethyl)amine (Me_6TREN) was synthesized according to literature procedures and stored at 4°C prior to use. Cyclodextrin initiator, mannose glycomonomer and heptamannose β -cyclodextrin (CD-Man_7) were synthesized as previously reported and stored at -20°C prior to use.^{21 22} All other reagents and solvents were purchased from Sigma Aldrich at the highest purity available and used without further purification unless stated otherwise.

2.2. Instrument and Analysis

Nuclear Magnetic Resonance (NMR)

Proton (^1H) Nuclear Magnetic Resonance ($^1\text{H-NMR}$) spectra were recorded on a 400 MHz Bruker Avance III spectrometer using $\text{DMSO-}d_6$, CDCl_3 , $\text{MeOD-}d_4$ or D_2O as the solvent at 300K. 2D Nuclear Overhauser Effect Spectroscopy (NOESY) NMR experiments were performed on a 600 MHz Bruker Avance NEO spectrometer in D_2O at a temperature of 303 K using the states-TPPI method with a 5ms Z-gradient spoil pulse in the mixing time and zero-quantum suppression using the method of M.J. Thrippleton & J.Keeler.²³ Mixing time was set to 0.3 s, spectra were recorded using 20 scans per t_1 increment and the spectral width was set to 8×8 ppm.

Dynamic Light Scattering (DLS)

The hydrodynamic diameters (D_h , the volume weight diameter of the distribution) evolution were determined characterized by a Malvern Zetasizer Nano ZS instrument equipped with a He-Ne laser at 633 nm. DLS measurements were performed by dissolving polymer samples at 1 mg/ml in deionized water and all the samples were passed through a $0.22 \mu\text{m}$ nylon filter before measurement. For complex samples, polymers were dissolved separately in deionized water and mixed together at different molar ratios. Then the samples were stirred

overnight at room temperature and filtered using a 0.22 nylon filter before analysis. All the samples were measured three times at 25 °C.

***In vitro* transfection and luciferase assay**

HEK 293T.17 cells (ATCC, USA) were plated at a density of 50,000 cells/well 48 hours prior to transfection. The polyplexes were added to each well in a total volume of 100 µL with a total dose of 100 ng of RNA in 20 mM HEPES with 5% glucose with n=3. The cells were then incubated with the polyplexes for 4 hours, and then the media was replaced with 100 µL of complete Dulbecco's Modified Eagle's Medium (cDMEM) (with 10% fetal bovine serum (FBS), 5 mg/mL L-glutamine, 5 mg/mL penicillin streptomycin (ThermoFisher, UK)). After 24 hours, 50 uL of media was removed and 50 uL of ONE-Glo™ luciferase substrate (Promega, UK) was added, and the total 100 µL was transferred to a white 96-well plate and analyzed on a FLUOstar Omega plate reader (BMG LABTECH, UK) with a gain of 4000. The average of the media only wells were subtracted from each sample measurement.

Human skin explant culture and digestion

Surgically resected specimens of human skin tissue were collected at Charing Cross Hospital, Imperial College London, UK. All tissues were collected after receiving signed, informed consent from all patients under protocols approved by the Local Research Ethics Committee. The tissue was obtained from patients undergoing elective abdominoplasty, breast reduction or mastectomy surgeries. Tissue was refrigerated until arrival in the laboratory. The subcutaneous layer of fat was completely removed, and the remaining skin layers were trimmed into ~1 cm² sections. Explants were cultured in 10 mL of cDMEM in a petri dish at 37 °C and 5% CO₂, and the media was refreshed daily.

Explants were injected with 2 µg of saRNA in a volume of 50 µL intradermally (ID) using a Micro-Fine Demi 0.3 mL syringe (Becton Dickinson, UK). After 3 days, skin was

digested as previously described.⁹ Briefly, explants were minced well with scissors and incubated in 2 mL DMEM supplemented with 1 mg/mL collagenase P (Sigma, UK) and 5 mg/mL dispase II (Sigma, UK) for 4 hours at 37°C on a rotational shaker. Digests were then filtered through a 70 µm cell strainer and centrifuged for 5 min at 1750 RPM. Cells were resuspended in 100 µL of FACS buffer (PBS + 2.5% FBS) and stained with 100 µL of Aqua Live/Dead Stain (ThermoFisher, UK) diluted 1:400 in FACS buffer for 20 min on ice. Cells were then washed with 1 mL of FACS buffer, centrifuged at 1750 RPM for 5 min and stained with a panel of antibodies (Supplementary Table 1) to identify cellular phenotypes for 30 minutes. Cells were then washed with 1 mL of FACS buffer, centrifuged at 1750 RPM for 5 minutes and resuspended in 250 µL of PBS. Cells were fixed with 250 µL of 3% paraformaldehyde for a total concentration of 1.5% and refrigerated until flow cytometry analysis.

Flow cytometry analysis

Single cell suspensions were analyzed on a LSRFortessa™ (BD Biosciences, UK) using FACSDiva software (BD Biosciences, UK) with 100,000 acquired events. Gating was performed as previously described.⁹ GFP⁺ cells and phenotypes were quantified using FlowJo Version 10 (FlowJo LLC, Oregon, USA).

Statistical analysis

Graphs and statistical analysis of *in vitro* and *ex vivo* data were prepared in GraphPad Prism, version 8.0. Statistical analysis was performed using a two-tailed t test or a one way ANOVA adjusted for multiple comparisons with $\alpha=0.05$ used to indicate significance.

2.3. Methods

General procedure for *ada*PEI synthesis

Linear polyethylene imine hydrochloride 40 kDa (PEI, 100 mg, 2.5×10^{-6} mol) was suspended in 40 mL dry CHCl_3 in a 100 mL RBF under Ar, equipped with stirring bar and sonicated for 30 min. Subsequently the suspension was stirred and 1 mL of dry TEA was added. Afterwards, the suspension was sonicated for 30 min until a fine suspension was achieved. A solution of adamantane carbonyl chloride (50 mg, 2.515×10^{-4} mol, 0.2 eq. per repeating unit) in 10 mL dry CHCl_3 was prepared and subsequently added to the suspension. The mixture was allowed to stir overnight at ambient temperature. After the reaction the suspension was filtered over the MilliPore and an NMR sample was taken in D_2O . Subsequently the filtered residue was dissolved in 10 mL H_2O to which 1 mL of a 32% HCl solution in water was added. The solution was subsequently precipitated in acetone and dried under vacuum. An NMR sample was taken in D_2O and average amount of adamantanes per chain were calculated by comparing the CH_2 - peak to the amount of adamantane protons. Quantities for synthesis of other *ada*PEIs can be found in **Table S1 and S2**.

SET-LRP polymerization of $\text{CD-}p(\text{Man}_8)_7$

A Schlenk tube was charged with CD_7 -initiator (10 mg, 2696.88 g/mol, 3.71 μmol), mannose glycomonomer (291 mg, 373.36 g/mol, 779 μmol , 30 eq. per initiating site), Me_6TREN (1.32 μL , 4.93 μmol , 0.19 eq. per initiating site), CuBr_2 (232 μg , 1.04 μmol , 1.04 eq. per initiating site) in DMSO (2 mL), sealed with a rubber septum and subsequently degassed by gentle bubbling of Ar gas for 15 min. The polymerization was then started by addition of pre-activated Cu(0) wire (5 cm) wrapped around a stirring bar under a positive Ar pressure and quickly sealed again and the reaction mixture was allowed to polymerize for 1 h at 25°C. Sampling was carried out using a degassed syringe to check the conversion of mannose glycomonomer. NMR samples was dissolved in $\text{DMSO-}d_6$ and conversion was determined as 27.5% (8.3 monomers per arm) by comparing the triazole peak to the vinyl protons. After polymerization the glycopolymer $\text{CD-}p(\text{Man}_8)_7$ was dialysed against water to remove excess

glycomonomer and further impurities. Molecular weight of the polymer was then determined *via* ^1H NMR and was revealed to be 24.5 kDa on average.

Synthesis of *glyco*PEI: Complexation of *ada*PEI with CD-Man₇

A solution of *ada*PEI2 (30.2 mg, 41088 g/mol, 0.734 μmol) and CD-Man₇ (17.9 mg, 2836.53 g/mol, 6.26 μmol , 8.58 eq. per polymer chain) was prepared in 10 mL H₂O amounting to a 1 / 1 ratio of cyclodextrin derivative per adamantane and sonicated until the solution became clear. Subsequently the solution was transferred to a 20 mL glass vial and freeze-dried. An NMR sample was made by dissolving 10 mg in D₂O for Nuclear Overhauser Effect Spectroscopy (NOESY). Quantities for synthesis of other *ada*PEIs can be found in **Table S1**.

Synthesis of *glyco*PEI: Complexation of *ada*PEI with CD-(pMan₈)₇

A solution of *ada*PEI1 (30.7 mg, 41390 g/mol, 0.741 μmol) and CD-(pMan₈)₇ (86 mg, 24499 g/mol, 3.51 μmol , 4.75 eq. per polymer chain) was prepared in 10 mL H₂O amounting to a 1 / 1 ratio of gycopolymer CD-(pMan₈)₇ per adamantane and sonicated until the solution became clear. Subsequently the solution was transferred to a 20 mL glass vial and freeze-dried.

saRNA synthesis and purification

Self-amplifying RNA encoding the non-structural proteins (NSPs) from the Venezuelan Equine Encephalitis Virus (VEEV) and either firefly luciferase (fLuc) or enhanced green fluorescent protein (eGFP) was prepared using *in vitro* transcription. pDNA was transformed into *Eschericia coli* and cultured in 50 mL of LB broth with 1 mg/mL carbenicillin (Sigma Aldrich, UK) and isolated using a Plasmid Plus Maxiprep kit (QIAGEN, UK). pDNA concentration and purifity were quantified on a NanoDrop One (ThermoFisher, UK) and then linearized using MluI for 3 h at 37 °C. Co-transcriptionally capped saRNA, used for *in vitro* experiments, was synthesized using 1 μg of linearized DNA template in a mMessage mMachin reaction (Ambion, UK) according to the manufacturer's protocol, and purified using

a MEGAclean column (Ambion, UK) according to the manufacturer's protocol. For *ex vivo* experiments, uncapped *in vitro* RNA transcripts were synthesized using 1 µg of linearized DNA template in a MEGAScript reaction (Ambion, UK) according to the manufacturer's protocol. Transcripts were then purified by overnight LiCl precipitation at -20 °C, pelleted by centrifugation at 14,000 RPM for 20 min at 4°C, washed with 70% EtOH, centrifuged at 14,000 RPM for 5 min at 4°C, and then resuspended in UltraPure H₂O. Purified transcripts were then capped using the ScriptCap™ and m⁷G Capping System (CellScript, Madison, WI, USA) and ScriptCap™ 2'-O-Methyltransferase Kit (CellScript, Madison, WI, USA) simultaneously according to the manufacturer's protocol. Capped transcripts were then purified again by LiCl precipitation and stored at -80 °C in a buffer of 10 mM HEPES with 100 mg/mL trehalose until use.

Particle complexation and characterization

Stock solutions of glycopolymers were prepared at a concentration of 5 mg/mL in ultrapure H₂O and purified using a 0.22 µm syringe filter (Millipore, Sigma, UK). saRNA complexes were prepared by mixing the RNA and polymer in 20 mM HEPES buffer (pH 7.4) with 5% glucose, with a ratio of polymer to RNA of 5:1 (w/w) unless otherwise specified. The solution was immediately vortexed for 30 seconds and then allowed to rest for 10 minutes prior to use.

Polyplexes were prepared in a volume of 800 µL of 20 mM HEPES with 5% glucose for particle size and charge analysis, and characterized on a Zetasizer NanoZS (Malvern Instruments, UK) with Zetasizer 7.1 software (Malvern Instruments, UK) in a clear disposable 1 mL cuvette. The polyplexes were analyzed using the following settings: a material refractive index of 1.529, absorbance of 0.010, dispersant viscosity of 0.8820 cP, refractive index of 1.330

and dielectric constant of 79. Each sample was analyzed three times for up to 100 runs or until the measurement stabilized.

Synthesis of per-(6-deoxy-6-bromine)- β -cyclodextrin (β -CD-(Br)₇)

Triphenylphosphine (Ph₃P, 36.72 g, 140 mmol) was dissolved in anhydrous DMF (150 mL) under stirring and cooled down to 0 °C (**Scheme S1**). *N*-bromosuccinimide (NBS, 24.92 g, 140 mmol) was dissolved in anhydrous DMF (40 mL) and the solution was added dropwise to the Ph₃P solution under Ar atmosphere and then stirred at ambient temperature for 30 min. β -Cyclodextrin (β -CD, 11.35 g, 10 mmol) (previously recrystallized three times from water and dried in vacuum oven at 50 °C for two days) was dissolved in anhydrous DMF (150 mL). The obtained Ph₃P/NBS solution was then added dropwise to the β -cyclodextrin solution at ambient temperature after which the solution temperature was increased to 80 °C. The mixed brown solution was stirred under Ar atmosphere overnight at 80 °C. Afterwards MeOH (40 mL) was added at ambient temperature and stirring was continued for 30 min. The reaction mixture was then cooled to 0 °C and the pH was adjusted to 9 by adding sodium methoxide, while further stirring for 1 h. The reaction mixture was then poured into stirred ice-water (4 L) resulting in a fine precipitate which was filtered and washed with MeOH. *Heptakis* (6-deoxy-6-bromo)- β -cyclodextrin was obtained as beige solids and dried under vacuum for 1 day. Yield: 11.32 g, 70%).

¹H NMR (400 MHz, DMSO-*d*₆, 298 K, ppm): δ = 6.02 (*d*, 7 H, 6.7 Hz), 5.89 (*d*, 7 H, 1.9 Hz), 4.98 (*d*, 7 H, 3.4 Hz), 4.00 (*d*, 7 H, 9.8 Hz), 3.82 (*t*, 7 H, 9.3 Hz), 3.65 (*m*, 14 H), 3.38 (*m*, 14 H, overlap with H₂O).

MALDI-TOF MS *m/z*: calculated for C₄₂H₆₃Br₇O₂₈K⁺: 1614.73; found, 1614.74.

Synthesis of per-(6-deoxy-6-azido)- β -cyclodextrin (β -CD-(N₃)₇)

Heptakis (6-deoxy-6-bromo)- β -cyclodextrin (10 g, 6.3 mmol) was dissolved in anhydrous DMF (80 mL) and NaN₃ (5.78 g, 88.8 mmol) (**Scheme S2**). The resulting suspension was stirred at 70 °C under Ar for 36 h. The suspension was then allowed to cool down and precipitated in 2 L of stirred ice-water. The precipitate was filtered, washed with water and redissolved in DMF (20 mL) and precipitated in 1L of stirred ice-water. The precipitate was filtered and washed with water and with little acetone. The resulting product was a white solid (yield: 7.2 g, 86.5 %) and was dried under vacuum overnight.

¹H NMR (400 MHz, DMSO-*d*₆, 298 K, ppm): δ = 5.90 (*d*, 7 H, 6.8 Hz), 5.75 (*d*, 7 H, 2 Hz), 4.91(*d*, 7 H, 3,4 Hz), 3.74 (*m*, 14 H), 3.59 (*m*, 14 H), 3.36 (*m*, 14 H, overlap with H₂O).

MALDI-TOF MS *m/z*: calculated for C₄₂H₆₃N₂₁O₂₈K⁺: 1348.37; found, 1348.27.

Synthesis of per-6-thio- β -cyclodextrin (β -CD-(SH)₇)

β -CD-(Br)₇ (5 g, 3.17 mmol) and thiourea (2.5 g, 33.3 mmol) were dissolved in DMF (50 mL) and the mixture was heated to 70 °C under argon atmosphere (**Scheme S3**). After 24 h, DMF was removed under reduced pressure and the obtained brown oil was dissolved in water (200 mL). Sodium hydroxide (2.22 g, 55.5 mmol) was then added and the reaction mixture was heated to a gentle reflux under nitrogen atmosphere. After 1 h, the resulting suspension was acidified with aqueous KHSO₄ forming a white precipitate which was then filtered and washed thoroughly with water and dried under vacuum. Compound β -CD-SH was recovered as white powder (yield: 3.2 g, 81%).

¹H NMR (400 MHz, DMSO-*d*₆, 298 K, ppm): δ = 5.91 (*d*, 7 H, 6.8 Hz), 5.81 (*d*, 7 H, 2 Hz), 4.93(*d*, 7 H, 3.3 Hz), 3.68 (*t*, 7 H, 8.5 Hz), 3.61 (*t*, 7 H, 9.2 Hz), 3.29-3.40 (*m*, 14 H, overlap with H₂O), 3.19 (*m*, 7H), 2.75 (*m*, 7 H), 2.13 (*t*, 7 H, 8.3 Hz).

Synthesis of allyl 2-bromoisobutyrate

Allyl alcohol (16.2 mL, 16.42 g, 282 mmol) and triethylamine (47.3 mL, 34.33 g, 339 mmol) were dissolved in diethyl ether (150 mL) and cooled down to 0 °C in an ice-water bath (**Scheme S4**). A solution of α -bromoisobutyryl bromide (BIBB) (27 mL, 50 g, 217 mmol) in 20 mL diethyl ether was added dropwise over a period of 20 min. The mixture was allowed to stir for 1 h at 0 °C after which it was allowed to reach room temperature and stirring was continued overnight. The solution was washed 3 x 50 mL 10% HCl solution, 3 x 50 mL 5% NaOH solution, 3 x 50 mL water and subsequently dried over MgSO₄. After evaporating the solvent via rotary evaporation, the product was purified by flash chromatography on silica gel using chloroform as an eluent affording a colourless oil. (yield: 76%, 23 g).

¹H NMR (400 MHz, CDCl₃, 298 K, ppm): δ = 5.9 (*ddt*, 1 H, 5.5 Hz, 10.6 Hz, 17.2 Hz), 5.35 (*dq*, 1 H, 1.5 Hz, 17.2 Hz), 5.24 (*dq*, 1 H, 1.3 Hz, 10.6 Hz), 4.63 (*dt*, 2 H, 1.4 Hz, 5.6 Hz), 1.91 (*s*, 6 H).

Synthesis of per-6-deoxy-6-(thiopropyl-2-bromo-2-methylpropanoate)- β -cyclodextrin

Per-6-thio- β -cyclodextrin (2.5 g, 2 mmol), and dithiothreitol (DTT, 618 mg, 4 mmol) were dissolved in 40 mL anhydrous DMF under Ar and heated to 60 °C (**Scheme S5**). After 60 h the reaction mixture was allowed to cool down to room temperature and allyl 2-bromoisobutyrate (14.53 g, 70 mmol), 2,2-dimethoxy-2-phenylacetophenone (DMPA, 179 mg, 7 mmol) were added to the reaction mixture and stirring was continued for 5 h under UV irradiation (365 nm).

The solution was precipitated in 500 mL of methyl tert-butyl ether (MTBE) in ten 50 mL centrifuge tubes and centrifuged at 8000 rpm for 5 min. The solvent was decanted and all precipitated fractions collected in two 50 mL centrifuge tubes and fresh MTBE was added, mixed and centrifuged again. This procedure was repeated 4 times in order to remove DMF

and allyl 2-bromoisobutyrate. Subsequently the product was dried under vacuum, yielding a fine beige solid. (3.7 g, yield: 68%).

^1H NMR (400 MHz, DMSO- d_6 , 298 K, ppm): δ = 5.90 (*d*, 7 H, 5.6 Hz), 5.8 (*m*, 7 H), 4.85 (*m*, 7 H), 4.22 (*t*, 14 H, 5.2 Hz), 3.85 (*m*, 7 H), 3.57 (*m*, 7 H), 3.33 (*m*, 14 H), 3.09 (*d*, 7 H, 10.6 Hz), 2.82 (*m*, 7 H), 2.69 (*m*, 14 H), 1.90 (*s*, 56 H).

MALDI-TOF MS m/z : calculated for $\text{C}_{91}\text{H}_{147}\text{Br}_7\text{O}_{42}\text{S}_7\text{K}^+$:2733.12; found: 2733.36.

Synthesis of 3-azido-propan-1-ol

3-bromopropan-1-ol (7 g, 50.35 mmol) was dissolved in a solution of acetone (250 mL) and water (50 mL) along with sodium azide (1.6 eq., 5.56 g, 86.61 mmol) and refluxed overnight at temperature of 70 °C (Scheme S6). The organic solvent was removed by rotary evaporation. 50 mL water was added to the remaining water phase and was then extracted with diethyl ether (3X50 mL). The resulting ether phase was then back extracted with water (50 mL) and dried over magnesium sulphate. The organic solvent was removed by rotary evaporation. The product was recovered as a colourless liquid and used directly (yield: 64%).

^1H NMR (400 MHz, D_2O , 298 K, ppm): δ = 3.66 (*t*, 2 H, 6.3 Hz), 4.41 (*t*, 2 H, 6.8 Hz), 1.81 (*quin*, 2 H, 6.5 Hz).

^{13}C NMR (100 MHz, D_2O , 298 K, ppm): δ = 58.78 (O- CH_2), 47.93 ($\text{CH}_2\text{-N}_3$), 30.49 (C- $\text{CH}_2\text{-C}$).

ESI-MS m/z : calcd for $\text{C}_6\text{H}_9\text{N}_3\text{O}_2$ ($2\text{M}+\text{H}^+$), 311.1; found, 311.1.

Notice: Organic azide is very sensitive compound and it should be handled with great care. After synthesis this intermediate was directly used for the next step reaction without further purification. Long period storage even in the fridge is not recommended.

Synthesis of 3-azidopropyl acrylate

A solution of 3-azido-propan-1-ol (6.10 g, 60.3 mmol), TEA (8.5 mL, 84.5 mmol), hydroquinone (30 mg) and anhydrous diethyl ether (200 mL) was cooled in an ice water bath (**Scheme S7**). Acryloyl chloride (5.88 mL, 72.4 mmol) in 20 mL diethyl ether was added dropwise into the solution. The mixture was stirred in the ice bath for 1 h and then at ambient temperature overnight. The ammonium salts were removed by filtration and the residue was extracted sequentially with aqueous solution of hydrochloric acid (10 v%, 3X50 mL), water (2X50 mL), 5 wt% aqueous NaOH (3X50 mL) and water (2X50 mL) and dried over magnesium sulphate. The organic solvent was removed by rotary evaporation. The product was recovered as a yellow liquid and used directly (yield: 45%).

¹H NMR (400 MHz, CDCl₃, 298 K, ppm): δ = 6.42 (*dd*, 1 H, 1.4, 17.3 Hz), 6.12 (*dd*, 1 H, 10.4, 17.3 Hz), 5.85 (*dd*, 1 H, 1.4, 10.4 Hz), 4.25 (*t*, 2 H, 6.2 Hz), 3.41 (*t*, 2 H, 6.7 Hz), 1.96 (*quin*, 2 H, 6.4 Hz).

Synthesis of 1-(2'-Propargyl) D-Mannose

1-(2'-Propargyl) D-Mannose was prepared according to the procedure reported by Mukhopadhyay *et al.*⁵⁴ A suspension solution of D-Mannose (12 g, 66.6 mmol), propargyl alcohol (19.4 mL, 333 mmol) and H₂SO₄-silica (333 mg) was stirred at 65 °C overnight (**Scheme S8**). After cooling to ambient temperature, the reaction mixture was transferred to a silica gel column and eluted with CHCl₃-MeOH (8:1) to remove the excess propargyl alcohol. 1-(2'-Propargyl) D-Mannose was obtained as a white solid after drying under vacuum (8 g, yield: 55 %). 1-(2'-propargyl) D-Mannose was found as an anomeric mixture in a ratio of 10:1 (α/β).

^1H NMR (400 MHz, CD_3OD , 298 K, ppm): δ : 4.96 (*d*, 1H, 1.6 Hz), 4.27 (*d*, 2H, 2.5 Hz), 3.84 (*dd*, 1H, 2.3, 11.8 Hz), 3.79 (*dd*, 1H, 1.8, 3.1 Hz), 3.66 (*m*, 3H), 3.51 (*m*, 1H), 2.85 (*t*, 1 H, 2.4 Hz)

Synthesis of D-Mannose glycomonomer

1-(2'-propargyl) D-mannose (2.46 g, 12.6 mmol) and 3-azidopropyl acrylate (2.85 g, 11.8 mmol) were dissolved in MeOH/ H_2O (2:1 vol/vol, 60 mL), aqueous solution of $\text{CuSO}_4 \cdot 5\text{H}_2\text{O}$ (246 mg, 0.9 mmol) and (+)-sodium L-ascorbate (284 mg, 1.2 mmol) were added into the reaction solution (). The reaction mixture was stirred at ambient temperature for 24 h and then the methanol was removed under vacuum and residue mixture was freeze dried to remove water. The purification of the obtained product was done by silica gel column chromatography using dichloromethane-MeOH (8:1) as eluent. After the removing of solvent, the product was obtained as white (1.62 g, yield: 58.2%).

^1H NMR (D_2O , 298 K, 400 MHz): δ = 8.07, 8.06 (s, overlapped, 1 H, $\text{NCH}=\text{C}$), 6.37 (dd, $J=1.8$, 15.5 Hz), 6.36 (dd, $J=1.6$, 15.7 Hz) (anomeric 1 H, $\text{CH}_2=\text{C}$), 6.14 (dd, $J=10.4$, 6.9 Hz), 6.13 (dd, $J=10.4$, 7.0 Hz) (anomeric, 1 H, $\text{CH}_2=\text{CHC}=\text{O}$), 5.89 (dd, 1 H, $J=1.5$, 8.9 Hz, $\text{CH}_2=\text{C}$), 4.70-5.05 (m, $\text{CH}_2\text{-OH}$, H-1 of mannose, overlap with H_2O), 4.64 (d, 1 H, $J=12.3$ Hz, $\text{CH}_2\text{-OH}$), 4.55 (t, 2 H, $J=6.9$ Hz, $\text{CH}_2\text{-N}$), 4.19 (t, 2 H, $J=6.0$ Hz, $\text{C}=\text{O}-\text{O}-\text{CH}_2$), 3.40-3.92 (m, H residues of mannose), 2.30 (m, 2H, $\text{CH}_2\text{-CH}_2\text{-CH}_2$) ppm.

^{13}C NMR (D_2O , 298 K, 400 MHz): δ = 146.4 ($\text{C}=\text{O}$), 145.4 ($\text{N}-\text{CH}=\text{C}$), 131.9 ($\text{CH}_2=\text{C}$), 129.2 ($\text{CH}_2=\text{C}$), 125.6 ($\text{N}-\text{CH}=\text{C}$), 100.8 (β anomeric, C1 of mannose), 100.7 (α anomeric, C 1 of mannose), 78.4, 75.2, 75.0, 72.5, 72.3, 72.0, 68.6, 68.4 (carbons of anomeric mannose), 63.0 ($\text{CH}_2\text{-OH}$), 62.6 ($\text{C}=\text{O}-\text{O}-\text{CH}_2$), 60.7 ($\text{C}-\text{CH}_2\text{-O}$), 48.5 ($\text{CH}_2\text{-CH}_2\text{-N}$), 28.5 ($\text{CH}_2\text{-CH}_2\text{-CH}_2$) ppm.

ESI-MS m/z : calcd for $\text{C}_{15}\text{H}_{23}\text{N}_3\text{O}_8$ ($\text{M}+\text{Na}^+$), 396.1; found, 396.1.

Synthesis of heptamannose β -cyclodextrin (CD-(Man)₇).

β -CD-(N₃)₇ (1.96 g, 1.5 mmol), 1-(2'-propargyl)-D-Mannose (2.61 g, 12 mmol) were dissolved in DMSO (20 mL) in a Schlenk tube (**Scheme S10**). Bipyridine (0.37 g, 0.0024 mmol) and CuBr (0.17 g, 0.0012 mmol) were added. The resulting mixture was evacuated and filled with argon and 3 freeze-pump-thaw cycles were performed to eliminate oxygen from the reaction mixture. The mixture was then allowed to stir at 50 °C for 24 h. After the reaction, water was added to the reaction medium and the resulting mixture was dialysed against water. After dialysis, the resulting clear solution was freeze dried.

¹H NMR (DMSO-d₆, 298 K, 400 MHz): δ = 7.95, 7.92 (s, overlapped, 7 H, NCH=C), 5.80-6.10 (m, 14 H, OH-2, OH-3 of CD), 5.10 (s, 7 H, H-1), 3.00-5.00 (m, CD & mannose residues, overlap with H₂O) ppm.

3. RESULTS AND DISCUSSION

3.1 Preparation and Characterization of Mannosylated PEI Polymers

A library of different PEI based polymers were successfully modified to contain appending adamantane units along the backbone. For this, commercially available PEI was first deprotonated using triethylamine and subsequently reacted with 1-adamantane carbonyl chloride *via* a simple substitution reaction (**Figure 1A**). The resulting *ada*PEI polymers were protonated and furthermore characterized using ¹H-NMR (**Figure 1B**) in order to determine the average adamantane content per polymer chain together with the change in molecular weight (**Table 1**). Protonation shifts PEI peak (-CH₂-CH₂-) from around 3.0 ppm to around 3.5 ppm. Percentages are defined as the percentage of monomer units along the polymer backbone. ¹H- NMR analysis revealed that there is a huge discrepancy between the amount of adamantyl groups added to the reaction and adamantyl actually found along the polymer chain.

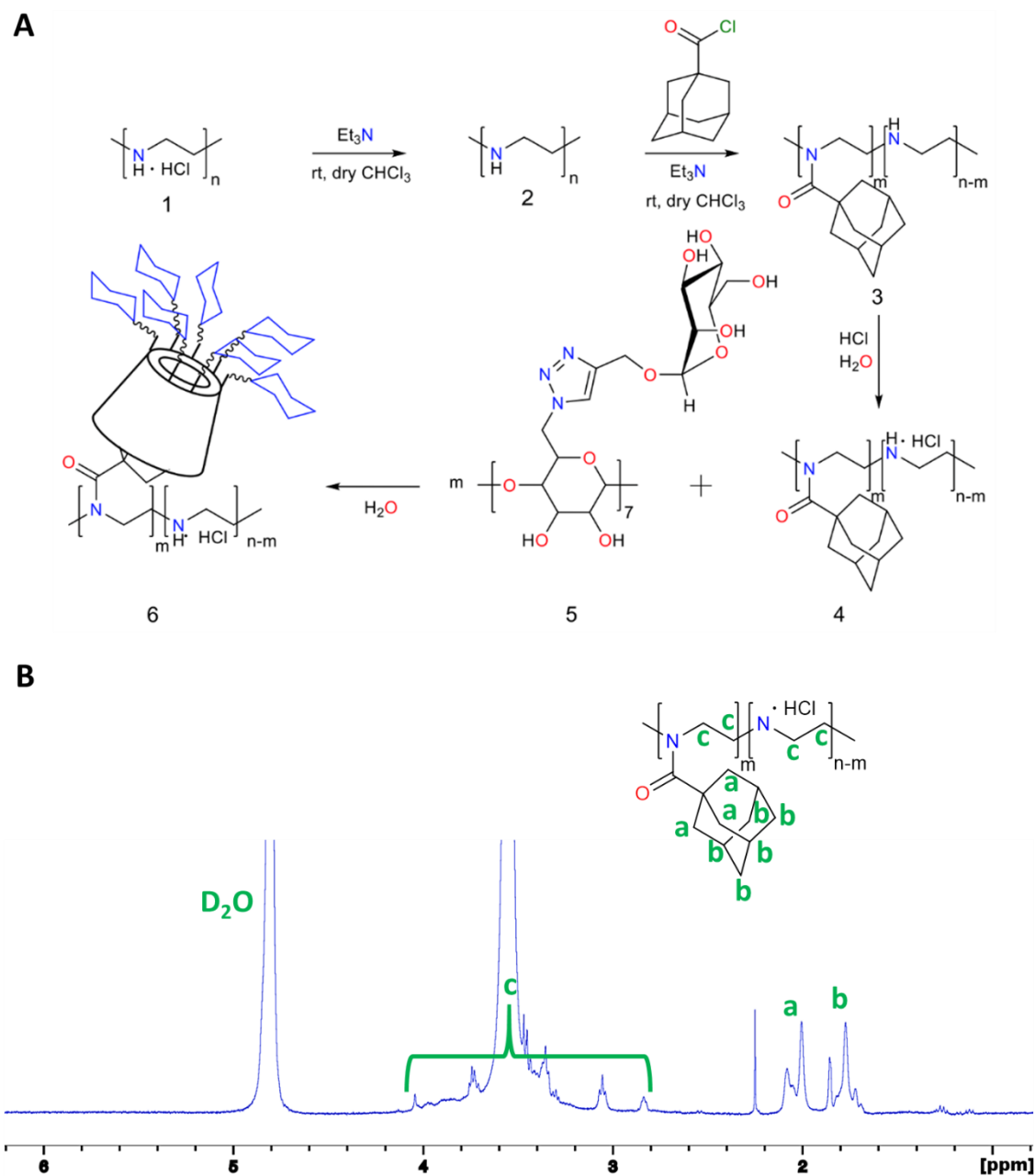


Figure 1. Chemical reaction scheme for the synthesis of *adaPEI* (4) and *glycoPEI* (6) (A); 1H NMR characterization of the synthesized *adaPEI*1 (B).

Apart from a monodisperse heptamannose β -cyclodextrin (CD-Man₇) previously synthesized within the group, a cyclodextrin based star-shaped mannose polymer was also prepared. Mannose monomer was synthesised as previously reported (analysis provided in ESI) and subsequently used for polymerisation starting from a heptavalent β -cyclodextrin based

initiator.^{21, 22} The polymerisation proceeded *via* Single Electron Transfer-Living Radical Polymerisation (SET-LRP) in DMSO for 1h and was followed *via* ¹H-NMR.

Table 1. Characteristics of the synthesized *glyco*PEI polymers before supramolecular interaction and after the supramolecular interaction.

<i>glyco</i> PEI	% Adamantane ^a	% Adamantane ^b	# Adamantanes per chain ^c	$M_{n, Theo}$ <i>ada</i> PEI ^d (Da)	$M_{n, Theo}$ <i>glyco</i> PEI ^e (Da)
PEI ₁	40	2.18	10.96	41390	72560
PEI ₂	20	1.71	8.58	41080	65480
PEI ₃	10	0.94	4.76	40600	54090
PEI ₄	5	0.54	2.72	40340	48060
PEI ₅	2.5	0.37	1.83	40230	45440
PEI ₆	1.25	0.14	0.71	40090	42110
PEI ₇	10	0.94	4.76	40600	157110
PEI	0	0	0	40000	-

^aTheoretical amount of adamantane before the reaction; ^bThe amount of adamantane according to ¹H NMR after the reaction; ^cThe number of adamantane per chain according to ¹H NMR; ^dThe molecular weight of the polymers according to ¹H NMR after the reaction; ^eThe molecular weight of the polymers according to ¹H NMR after the complexation with CD.

The resulting *ada*PEIs were subsequently mannosylated in a supramolecular manner by combining the *ada*PEIs with CD-Man₇ or CD-(*p*Man₈)₇ in water. The resulting *glyco*PEIs were then characterized *via* ¹H-NMR, 2D NOESY NMR and DLS which confirmed the anticipated host-guest complexation between the adamantyl groups and CD-Man₇ as NOESY experiments revealed cross-peaks between the signals at 4 – 4.3 ppm assigned to the inner protons of the CD-Man₇ cavity and the signals at 1.9 – 2.4 ppm assigned to the adamantane not present when taken 2D NOESY from the respective pure products (**Figure 2A**). Additionally, as seen in **Figure 2B**, the host-guest interaction between PEI₁ and CD-Man₇ was further confirmed by DLS, which revealed that size and size distribution increased due to the attachment of

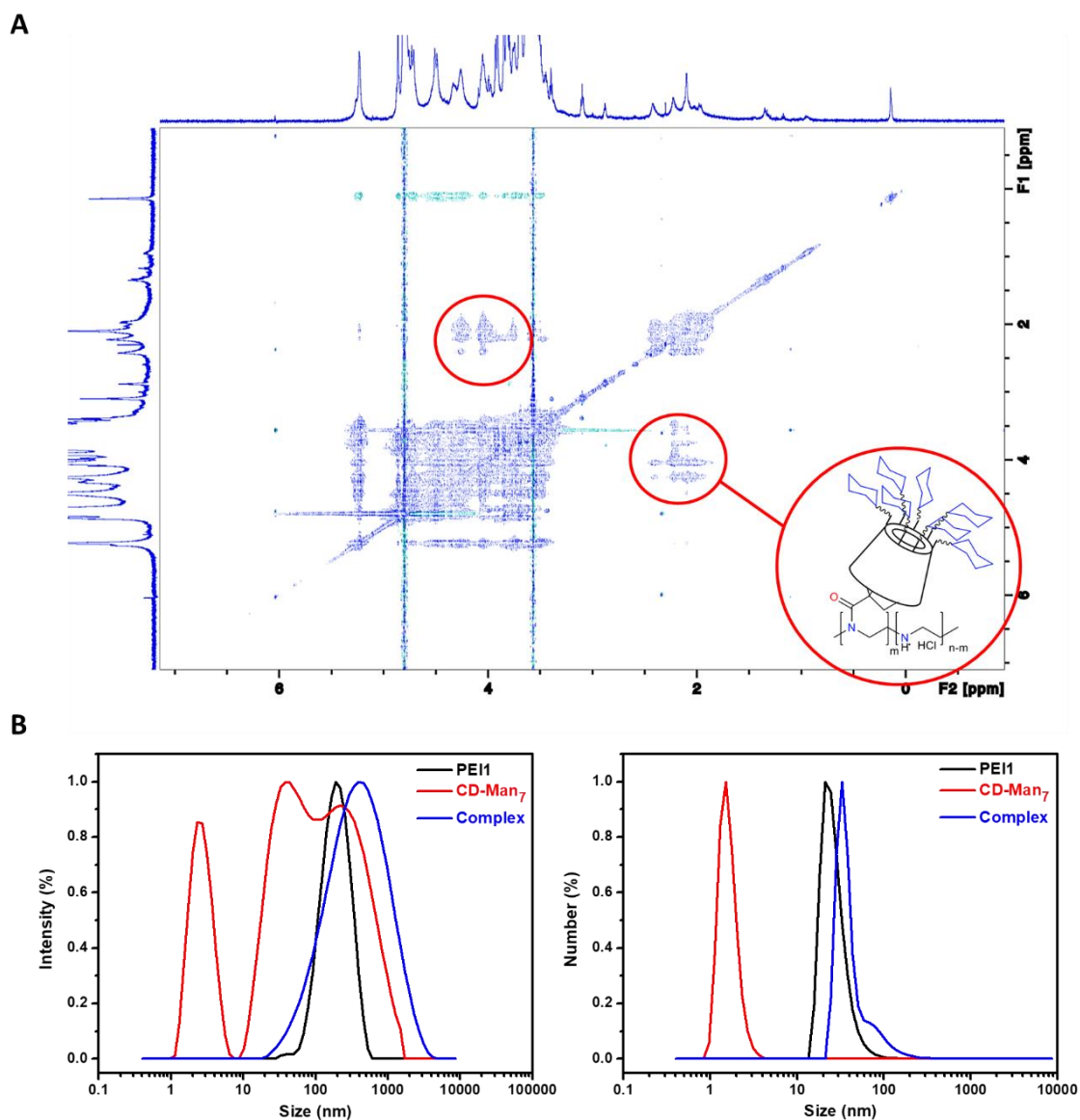


Figure 2. 2D NOESY-NMR spectrum of the *ada*PEI1 and CD-Man₇, clearly showing cross peaks between the signals at 4.0 – 4.3 ppm assigned to the inner protons of the CD-Man₇ cavity and the signals at 1.9 – 2.4 ppm assigned to the adamantane (A); DLS measurements of the *ada*PEI1 and CD-Man₇ before and after supramolecular interaction (B).

CD-Man₇ on the backbone of PEI1. The mean hydrodynamic size of PEI1 increased dramatically from 125 nm to 218 nm while distribution index increased from 0.34 to 0.58 after the host-guest complexation. Besides, large aggregates of CD-Man₇ disappeared after the complexation, which also proved that the interaction of CD-Man₇ with adamantane units on

the polymer backbone could eliminate the formation of interchain assemblies or aggregations. The resulting solutions were furthermore freeze-dried, resulting in a fine powder which is easily dissolvable for use in RNA transfection.

3.2 Preparation and Characterization of saRNA/ManPEI Polyplexes In Vitro

Particle size and charge were characterized after complexation with saRNA (**Figure 3**). All particles were found to be between 50-200 nm in size, with a slight trend of increasing size with increasing degree of mannosylation. All particles were positively charged after saRNA complexation, indicating that the host-guest interaction does not interfere with the cationic charges or further condensation of saRNA molecules.

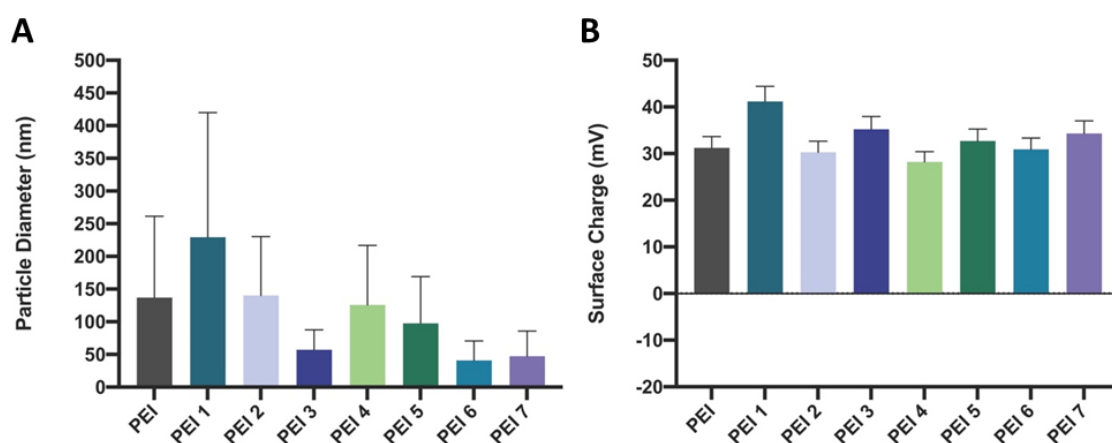


Figure 3. Particle size and zeta potential of PEI-Ad-CD-Man₇/saRNA polyplexes as determined by DLS. Z-average particle diameter (the volume weight diameter of the distribution) (**A**) and zeta potential (**B**) of complexes prepared at a ratio of 5:1 polymer to RNA (w/w). Bars represent mean \pm standard deviation for n=3.

In order to investigate the effects of the ratio of PEI to saRNA and degree of mannosylation on transfection efficiency *in vitro*, we prepared polyplexes with saRNA and PEI polymers with and without mannosylation. We observed how the degree of mannosylation affected transfection efficiency, using either unmodified PEI, PEI with varying amounts of

Man₇ (PEI₁₋₆) or PEI with polyMan₇ (PEI₇) (**Figure 4A**). Because changing the mass ratio of polymer to saRNA changes the amount of available positively charged amines, we used a fixed ratio of PEI to saRNA of 5:1 (w/w) and then normalized the molar amount of PEI in each formulation for PEI₁₋₇. We observed that PEI had the highest transfection efficiency, ~10⁶ RLU, whereas all of the mannosylated PEIs were lower, between 1-5x10⁵ RLU. In addition, increasing the degree of mannosylation decreased the transfection efficiency *in vitro*, as PEI₄₋₆ had the highest transfection efficiency of the mannosylated PEIs, and PEI₁₋₃ had the lowest. We hypothesize that this is due to steric hinderance cause by increasing degree of mannosylation which may limit the access that saRNA has to the amine groups on PEI.

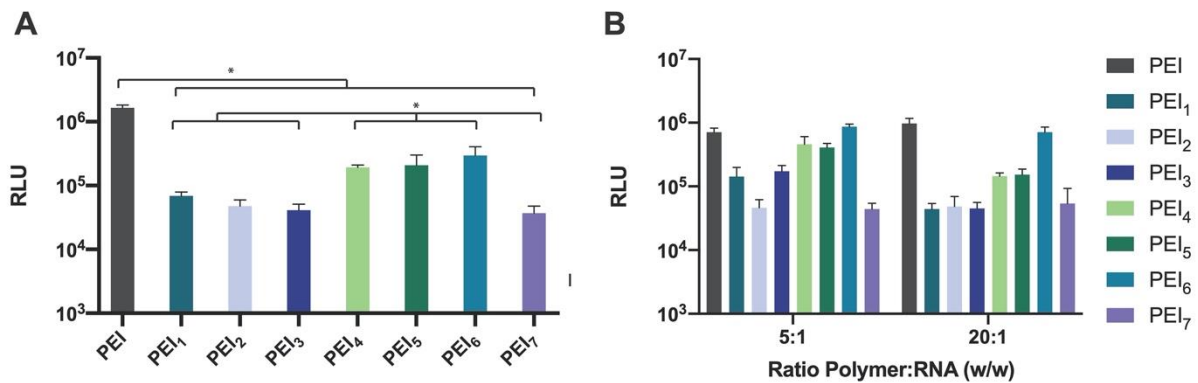


Figure 4. In vitro transfection efficiency of PEI-Ad-CD-Man₇ complexes with fLuc saRNA in HEK293T.17 cells after 24 hours. Transfection efficiency with formulations normalized to the molar amount of PEI in the complex (**A**); Transfection efficiency with formulations prepare by varying ratio of polymer to RNA. Bars represent mean ± standard deviation for n=3 (**B**).

Furthermore, while HEK cells can be induced to express the mannose receptor,²⁴ they do not naturally express it, thus these experiments exhibit how the structure of the polyplexes affects non-mannose mediated uptake. Furthermore, we observed similar transfection efficiency between the 5:1 and 20:1 ratios of polymer to saRNA (w/w) *in vitro* (**Figure 4B**). This is most likely due to glycopolymers being saturated with saRNA even at lower ratios of polymer to RNA, which is supported by the Zetasizer data (**Figure 3**) wherein even at a ratio

of 5:1, the particles exhibit a positive charge. Thus, adding more polymer does not increase the transfection efficiency. Overall, we observed that increasing the degree of mannosylation, but not the ratio of mannosylated PEI to saRNA, decreased the transfection efficiency *in vitro*.

3.3 Transfection Efficiency of saRNA/ManPEI Polyplexes in Human Skin Explants.

Because *in vitro* transfection efficiency does not generally correlate well with *in vivo* efficacy,²⁵ we sought to test these glycopolymers in a clinically translational human skin explant model. Human skin explants have previously been shown to be a viable model for optimization of nucleic acid formulations,⁹ and contain many cell types with the mannose receptor including dendritic cells, fibroblasts, and macrophages.²⁶⁻³⁰ We first prepared formulations with either RNA alone, PEI or mannosylated PEI (PEI₁₋₆) (**Figure 5A**) at a ratio of 5:1 polymer to saRNA (w/w). We were surprised to observe that the polyplexes did not enhance the percentage of eGFP⁺ in skin explants, even with unmodified PEI (**Figure S6A**). We observed a similar effect for PEI with polyMan₇- only ~1% of cells expressed GFP and there was no observed benefit to naked RNA alone (**Figure S6B**). We then tested whether increasing the ratio of PEI₁ to saRNA had any effect on the percentage of cells expressing GFP (**Figure 5B**). We observed that increasing the ratio of PEI₁ to saRNA to 10:1 and 20:1 (w/w) did indeed increase the number of GFP⁺ cells to 5% and 8%, with p=0.018 and 0.00038, respectively. This enhancement is superior to previously studied LNP formulations.⁹

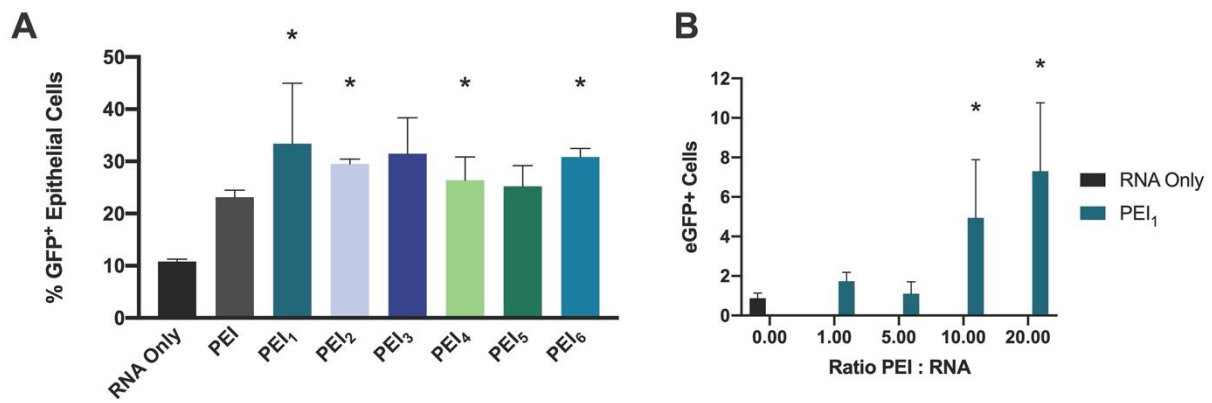


Figure 5. Ex vivo transfection efficiency in human skin explants. Percentage of eGFP⁺ epithelial cells in human skin explants after ID injection of saRNA/ PEI-Ad-CD-Man₇ complexes prepared at a ratio of 20:1 (w/w) after 72 hours in culture. Bars represent mean \pm standard deviation for n=3. * indicates significance of p<0.05 (A); Percentage of eGFP⁺ cells in human skin explants after treatment with saRNA/PEI-Ad-CD-Man₇ complexes after 72 hours in culture. The ratio of complexes to RNA was varied from 1:1 to 20:1 (w/w) of PEI₁. Bars represent the mean \pm standard deviation for n=3. * indicates significance of p<0.05 compared to RNA only(B).

3.4 Impact of Ratio of ManPEI to saRNA on Ex Vivo Phenotypic Protein Expression

We then characterized which cells were expressing the saRNA using a flow cytometry panel capable of identifying epithelial cells (CD45⁻), fibroblasts (CD90⁺), NK cells (CD56⁺), leukocytes (CD45⁺), Langerhans cells (CD1a⁺), monocytes (CD14⁺) dendritic cells (CD11c⁺), T cells (CD3⁺) and B cells (CD19⁺). As previously observed, the majority of cells that make up the skin are epithelial cells, fibroblasts and dendritic cells, and leukocytes, Langerhans cells, B cells, monocytes and T cells to a lesser extent (**Figure 6A**). While epithelial cells make up ~64% of the total cells, they make up only 16% of the cells expressing the saRNA alone. However, when the saRNA was complexed with mannosylated PEI₁ at a ratio of 20:1

(w/w), it was expressed in ~33% of epithelial cells (**Figure 6B**). GFP was expressed in either a similar or lesser percentage of the other cell types. Overall, we observed that increasing the ratio of mannosylated PEI to saRNA increased the number of cells expressing saRNA in human skin explants, and we identified that epithelial cells were specifically targeted by these polyplexes.

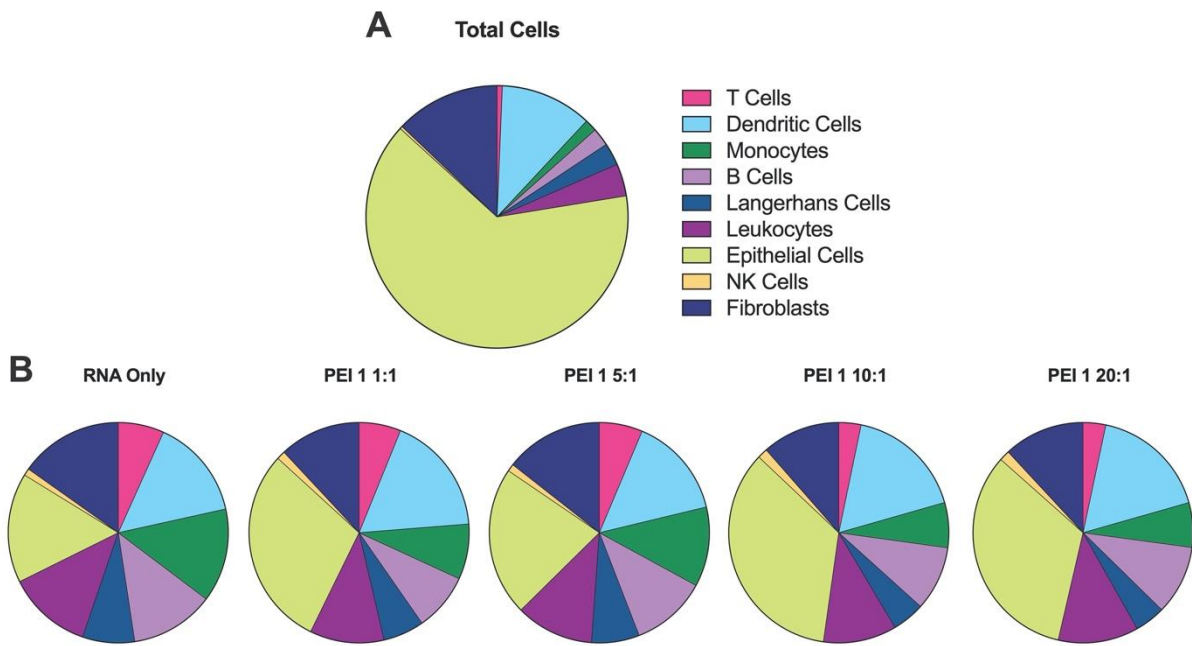


Figure 6. Phenotypic identity of eGFP⁺ cells in human skin explants alone (**A**) and after ID injection of GFP saRNA/PEI-Ad-CD-Man₇ complexes at varying ratios of PEI₁ to saRNA (**B**). Cells were identified using the following antibodies: epithelial cells (CD45⁻), fibroblasts (CD90⁺), NK cells (CD56⁺), leukocytes (CD45⁺), Langerhans cells (CD1a⁺), monocytes (CD14⁺), dendritic cells (CD11c⁺), T cells (CD3⁺) and B cells (CD19⁺).

3.5 Impact of Degree of Mannosylation on Phenotypic Expression of saRNA Ex Vivo

Given our observation that increasing the ratio of mannosylated PEI to saRNA enhanced the number of cells expressing saRNA, we then studied whether the degree of mannosylation affected cellular uptake and expression *ex vivo* (**Figure 7**). We prepared polyplexes at a fixed ratio of 20:1 (w/w) of PEI to saRNA and again evaluated which cells were expressing GFP. We observed that at a ratio of 20:1, the PEI formulations (both unmodified and mannosylated) increased the percentage of GFP⁺ cells to ~8%. Increasing the degree of mannosylation had a trend of increasing the percentage of epithelial cells expressing GFP (**Figure 7**), although only the PEI_{1,2,4,6} groups were found to be statistically significantly higher. While the mannose receptor is primarily known to be expressed by macrophages, dendritic cells, fibroblasts and keratinocytes, it has previously been shown to be expressed by vaginal epithelial cells.³¹ It is possible that human skin epithelial cells also express the mannose receptor, leading to increased polyplex uptake and saRNA expression in these cells. However, in these studies we quantified the percentage of cells *expressing* the saRNA, not the percentage of cellular uptake, so it is possible that there is increased uptake into cells that are known to express the mannose receptor. In the context of RNA vaccines, it has yet to be defined as to which cells are desired to express the protein; we hypothesize that an increased protein expression will result in increased immunogenicity. Overall, we show that increasing the degree of mannosylation increases protein expression, specifically in epithelial cells of human skin explants.

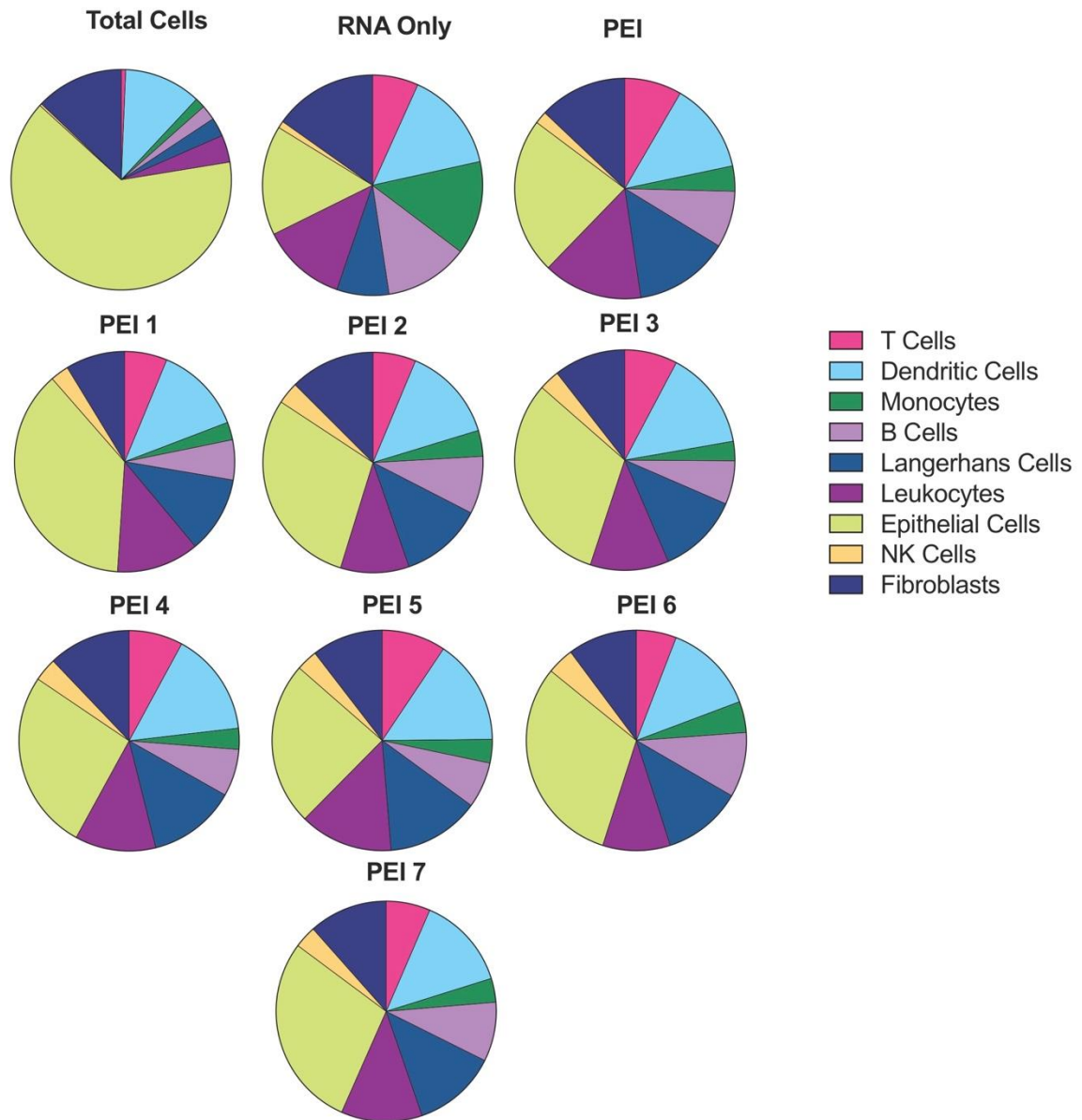


Figure 7. Phenotypic identity of eGFP⁺ cells in human skin explants after ID injection of saRNA/PEI-Ad-CD-Man₇ complexes prepared at a ratio of 20:1 (w/w) with PEI₁₋₇ after 72 hours in culture. Cells were identified using the following antibodies: epithelial cells (CD45⁻), fibroblasts (CD90⁺), NK cells (CD56⁺), leukocytes (CD45⁺), Langerhans cells (CD1a⁺), monocytes (CD14⁺), dendritic cells (CD11c⁺), T cells (CD3⁺) and B cells (CD19⁺).

4. CONCLUSION

A library of mannosylated PEI polymers enabled by the host-guest interaction between cyclodextrin and adamantane for targeted saRNA delivery was investigated. We show that while increasing the degree of mannosylation stifles *in vitro* transfection efficiency, it enhances the percentage of cells expressing the saRNA in human skin explants. Furthermore, it was investigated that increasing the ratio of polymer to saRNA also enhanced the protein expression *ex vivo*, which was specifically due to an increase in epithelial cell expression. Meanwhile, increasing the degree of mannosylation also increased expression specifically in epithelial cells. We believe that this platform, which enables glycosylation of PEI through host-guest chemistry, is a highly clinically translational delivery vehicle and is dually useful for targeting specific cell types for saRNA delivery and expression.

ASSOCIATED CONTENT

Supporting Information.

Experimental details for the synthesis of all compounds are provided in the ESI.

AUTHOR INFORMATION

Corresponding Author

Remzi.Becer@warwick.ac.uk and R.Shattock@imperial.ac.uk

Author Contributions

The manuscript was written through contributions of all authors. All authors have given approval to the final version of the manuscript. ‡These authors contributed equally.

Acknowledgements

We gratefully acknowledge the surgeons (Elizabeth A. Dex and Judith E. Hunter) and their nursing team at Charing Cross Hospital. We also acknowledge Dormeur Investment Services Ltd for providing funds to purchase equipment used in these studies. AKB is supported by a Whitaker Post-Doctoral Fellowship and a Marie Skłodowska Curie Individual Fellowship funded by the European Commission H2020 (No. 794059). PFM, CRB, and RJS are funded by the U.K. Department of Health and Social Care through the Future Vaccine Manufacturing Hub through the Engineering and Physical Sciences Research Council (EPSRC, grant number: EP/R013764/1). This project has received funding from the European Union's Horizon 2020 research and innovation programme under the Marie Skłodowska-Curie grant agreement No 642083. RL acknowledge the China Scholarship Council (CSC) and Queen Mary, University of London for funding this project.

5. REFERENCES

1. Perri, S.; Greer, C. E.; Thudium, K.; Doe, B.; Legg, H.; Liu, H.; Romero, R. E.; Tang, Z.; Bin, Q.; Dubensky, T. W.; Vajdy, M.; Otten, G. R.; Polo, J. M., An Alphavirus Replicon Particle Chimera Derived from Venezuelan Equine Encephalitis and Sindbis Viruses Is a Potent Gene-Based Vaccine Delivery Vector. *J. Virol.* **2003**, *77*, (19), 10394-10403.
2. Chahal, J. S.; Khan, O. F.; Cooper, C. L.; McPartlan, J. S.; Tsosie, J. K.; Tilley, L. D.; Sidik, S. M.; Lourido, S.; Langer, R.; Bavari, S.; Ploegh, H. L.; Anderson, D. G., Dendrimer-RNA nanoparticles generate protective immunity against lethal Ebola, H1N1 influenza, and *Toxoplasma gondii* challenges with a single dose. *Proc. Natl. Acad. Sci. U. S. A.* **2016**, *113*, (29), E4133-E4142.
3. Geall, A. J.; Verma, A.; Otten, G. R.; Shaw, C. A.; Hekele, A.; Banerjee, K.; Cu, Y.; Beard, C. W.; Brito, L. A.; Krucker, T.; O'Hagan, D. T.; Singh, M.; Mason, P. W.; Valiante, M. N.; Dormitzer, P. R.; Barnett, S. W.; Rappuoli, R.; Ulmer, J. B.; Mandl, C. W., Nonviral delivery of self-amplifying RNA vaccines. *Proc. Natl. Acad. Sci. U. S. A.* **2012**, *109*, (36), 14604-14609.
4. Bogers, W. M.; Oostermeijer, H.; Mooij, P.; Koopman, G.; Verschoor, E. J.; Davis, D.; Ulmer, J. B.; Brito, L. A.; Cu, Y.; Banerjee, K.; Otten, G. R.; Burke, B.; Dey, A.; Heeney, J. L.; Shen, X.; Tomaras, G. D.; Labranche, C.; Montefiori, D. C.; Liao, H. X.; Haynes, B.; Geall, A. J.; Barnett, S. W.,

Potent immune responses in rhesus macaques induced by non-viral delivery of a self-amplifying RNA vaccine expressing HIV-1 envelope with a cationic nanoemulsion. *J. Infect. Dis.* **2015**, 211, (6), 947-955.

5. Evans, C. F.; Dolter, K. E.; Song, J.; Luxembourg, A.; Bernard, R.; Hannaman, D., 240. Risk of Insertional Mutagenesis Following In Vivo Transfer of Plasmid DNA: Role of Host Immune Responses. *Mol. Ther.* **2008**, 16, S91.

6. Pardi, N.; Hogan, M. J.; Porter, F. W.; Weissman, D., mRNA vaccines — a new era in vaccinology. *Nat. Rev. Drug Discovery* **2018**, 17, (4), 261-279.

7. Lundstrom, K., Replicon RNA Viral Vectors as Vaccines. *Vaccines* **2016**, 4, (4), 39.

8. McCullough, K. C.; Bassi, I.; Milona, P.; Suter, R.; Thomann-Harwood, L.; Englezou, P.; Démoulin, T.; Ruggli, N., Self-replicating Replicon-RNA Delivery to Dendritic Cells by Chitosan-nanoparticles for Translation In Vitro and In Vivo. *Mol. Ther.--Nucleic Acids* **2014**, 3, e173.

9. Blakney, A. K.; McKay, P. F.; Ibarzo Yus, B.; Hunter, J. E.; Dex, E. A.; Shattock, R. J., The Skin You Are In: Design-of-Experiments Optimization of Lipid Nanoparticle Self-Amplifying RNA Formulations in Human Skin Explants. *ACS Nano* **2019**, 13, (5), 5920-5930.

10. Démoulin, T.; Milona, P.; Englezou, P. C.; Ebensen, T.; Schulze, K.; Suter, R.; Pichon, C.; Midoux, P.; Guzmán, C. A.; Ruggli, N.; McCullough, K. C., Polyethylenimine-based polyplex delivery of self-replicating RNA vaccines. *Nanomedicine* **2016**, 12, (3), 711-722.

11. Blakney, A. K.; Yilmaz, G.; McKay, P. F.; Becer, C. R.; Shattock, R. J., One Size Does Not Fit All: The Effect of Chain Length and Charge Density of Poly(ethylene imine) Based Copolymers on Delivery of pDNA, mRNA, and RepRNA Polyplexes. *Biomacromolecules* **2018**, 19, (7), 2870-2879.

12. Chahal, J. S.; Khan, O. F.; Cooper, C. L.; McPartlan, J. S.; Tsosie, J. K.; Tilley, L. D.; Sidik, S. M.; Lourido, S.; Langer, R.; Bavari, S.; Ploegh, H. L.; Anderson, D. G., Dendrimer-RNA nanoparticles generate protective immunity against lethal Ebola, H1N1 influenza, and *Toxoplasma gondii* challenges with a single dose. *PNAS* **2016**, 113, (29), E4133.

13. Liang, F.; Lindgren, G.; Lin, A.; Thompson, E. A.; Ols, S.; Röhss, J.; John, S.; Hassett, K.; Yuzhakov, O.; Bahl, K.; Brito, L. A.; Salter, H.; Ciaramella, G.; Loré, K., Efficient Targeting and Activation of Antigen-Presenting Cells In Vivo after Modified mRNA Vaccine Administration in Rhesus Macaques. *Mol. Ther.* **2017**, 25, (12), 2635-2647.

14. Veiga, N.; Goldsmith, M.; Granot, Y.; Rosenblum, D.; Dammes, N.; Kedmi, R.; Ramishetti, S.; Peer, D., Cell specific delivery of modified mRNA expressing therapeutic proteins to leukocytes. *Nat. Commun.* **2018**, 9, (1), 4493.

15. Willoughby, J. L. S.; Chan, A.; Sehgal, A.; Butler, J. S.; Nair, J. K.; Racie, T.; Shulgamorskaya, S.; Nguyen, T.; Qian, K.; Yucius, K.; Charisse, K.; van Berkel, T. J. C.; Manoharan, M.; Rajeev, K. G.; Maier, M. A.; Jadhav, V.; Zimmermann, T. S., Evaluation of GalNAc-siRNA Conjugate Activity in Pre-clinical Animal Models with Reduced Asialoglycoprotein Receptor Expression. *Mol. Ther.* **2018**, 26, (1), 105-114.

16. Pun, S. H.; Bellocq, N. C.; Liu, A.; Jensen, G.; Machemer, T.; Quijano, E.; Schluep, T.; Wen, S.; Engler, H.; Heidel, J.; Davis, M. E., Cyclodextrin-Modified Polyethylenimine Polymers for Gene Delivery. *Bioconjugate Chem.* **2004**, 15, (4), 831-840.
17. Miyauchi, M.; Harada, A., Construction of Supramolecular Polymers with Alternating α -, β -Cyclodextrin Units Using Conformational Change Induced by Competitive Guests. *J. Am. Chem. Soc.* **2004**, 126, (37), 11418-11419.
18. Wang, J.; Jiang, M., Polymeric Self-Assembly into Micelles and Hollow Spheres with Multiscale Cavities Driven by Inclusion Complexation. *J. Am. Chem. Soc.* **2006**, 128, (11), 3703-3708.
19. Yilmaz, G.; Uzunova, V.; Napier, R.; Becer, C. R., Single-Chain Glycopolymer Folding via Host-Guest Interactions and Its Unprecedented Effect on DC-SIGN Binding. *Biomacromolecules* **2018**, 19, (7), 3040-3047.
20. Kauscher, U.; Ravoo, B. J., Mannose-decorated cyclodextrin vesicles: The interplay of multivalency and surface density in lectin-carbohydrate recognition. *Beilstein J. Org. Chem.* **2012**, 8, 1543-1551.
21. Abdouni, Y.; Yilmaz, G.; Becer, R., Sequence Controlled Polymers from a Novel β -Cyclodextrin Core. *Macromol. Rapid Commun.* **2017**; Vol. 38, p 1700501.
22. Oz, Y.; Abdouni, Y.; Yilmaz, G.; Becer, C. R.; Sanyal, A., Magnetic glyconanoparticles for selective lectin separation and purification. *Polym. Chem.* **2019**, 10, (24), 3351-3361.
23. J Thrippleton, M.; Keeler, J., Elimination of Zero-Quantum Interference in Two-Dimensional NMR Spectra. *Angew. Chem., Int. Ed.* **2003**, 42, 3938-41.
24. Vigerust, D. J.; Vick, S.; Shepherd, V. L., Stable Expression and Characterization of an Optimized Mannose Receptor. *J. Clin. Cell. Immunol.* **2015**, 6, (3), 330.
25. Hajj, K. A.; Ball, R. L.; Deluty, S. B.; Singh, S. R.; Strelkova, D.; Knapp, C. M.; Whitehead, K. A., Branched-Tail Lipid Nanoparticles Potently Deliver mRNA In Vivo due to Enhanced Ionization at Endosomal pH. *Small* **2019**, 15, (6), 1805097.
26. McKenzie, E. J.; Taylor, P. R.; Stillion, R. J.; Lucas, A. D.; Harris, J.; Gordon, S.; Martinez-Pomares, L., Mannose Receptor Expression and Function Define a New Population of Murine Dendritic Cells. *J. Immunol.* **2007**, 178, (8), 4975.
27. Wollenberg, A.; Oppel, T.; Schottdorf, E.-M.; Günther, S.; Moderer, M.; Mommaas, M., Expression and Function of the Mannose Receptor CD206 on Epidermal Dendritic Cells in Inflammatory Skin Diseases. *J. Invest. Dermatol.* **2002**, 118, (2), 327-334.
28. Hespanhol, R. C.; Soeiro, M. d. N. C.; Meuser, M. B.; Meirelles, M. d. N. S. L.; Côte-Real, S., The Expression of Mannose Receptors in Skin Fibroblast and Their Involvement in *Leishmania (L.) amazonensis* Invasion. *J. Histochem. Cytochem.* **2005**, 53, (1), 35-44.
29. Lee, S. H.; Charmoy, M.; Romano, A.; Paun, A.; Chaves, M. M.; Cope, F. O.; Ralph, D. A.; Sacks, D. L., Mannose receptor high, M2 dermal macrophages mediate nonhealing *Leishmania major* infection in a Th1 immune environment. *J. Exp. Med.* **2018**, 215, (1), 357.

30. Linehan, S. A., The mannose receptor is expressed by subsets of APC in non-lymphoid organs. *BMC Immunol.* **2005**, 6, 4-4.
31. Fanibunda, S. E.; Modi, D. N.; Gokral, J. S.; Bandivdekar, A. H., HIV gp120 Binds to Mannose Receptor on Vaginal Epithelial Cells and Induces Production of Matrix Metalloproteinases. *PLOS ONE* **2011**, 6, (11), e28014.